

# Ultimate Properties of Epoxy Resins Modified with a Polysiloxane–Polycaprolactone Block Copolymer

L. KÖNCZÖL,<sup>1,\*</sup> W. DÖLL,<sup>1</sup> U. BUCHHOLZ,<sup>2,†</sup> and R. MÜLHAUPT<sup>2</sup>

<sup>1</sup>Fraunhofer-Institut für Werkstoffmechanik, Wöhlerstr. 11, D-79108 Freiburg, Germany, and <sup>2</sup>Freiburger Materialforschungszentrum (FMF) und Institut für Makromolekulare, Chemie Hermann Staudinger Haus, Stefan-Meier-Str. 31, D-79104 Freiburg, Germany

## SYNOPSIS

Mechanical and fracture mechanics properties of transparent multiphase epoxy resins toughened with various amounts of compatibilized silicone liquid rubbers consisting of polycaprolactone-*block*-poly(dimethylsiloxane)-*block*-polycaprolactone triblock copolymer have been investigated. At silicone liquid rubber contents < 10 wt % significantly improved toughness has been achieved without adversely affecting thermal and mechanical properties. Fractographic and interferometric methods have been applied to study crack propagation in such silicone-modified resins. © 1994 John Wiley & Sons, Inc.

## INTRODUCTION

Highly crosslinked polymeric matrix materials such as epoxy resins are known for their high performance, especially with respect to thermal and dimensional stabilities combined with high stiffness and strength at low creep. As a consequence of their highly crosslinked structure, these materials tend to suffer from brittle behavior, poor crack resistance, and low fracture toughness. A well-known procedure to toughen such brittle polymers is to incorporate discrete rubber particles into the rigid matrix. Since the pioneering work at Goodrich Company, the carboxy-terminated butadiene acrylonitrile copolymers (CTBN) have been applied with great success to enhance toughness of epoxy resins or related matrix resins without sacrificing other useful properties such as dimensional stability, stiffness, and strength. The major drawback of the elastomeric butadiene backbone is its poor oxidative stability due to the high olefin content of the polymer backbone.

Silicone rubbers, especially poly(dimethylsiloxane) (PDMS), exhibit a number of attractive properties: high chain flexibility and low intermo-

lecular forces responsible for an extremely low glass transition temperature ( $-123^{\circ}\text{C}$ ), low surface tension and surface energy, low solubility parameters, and hydrophobic behavior. In addition, PDMS shows ultraviolet (UV) insensitivity, oxygen, and temperature stability. This combination of excellent features provides the necessary conditions for the application of PDMS as elastomeric modifier exhibiting both good phase separation and high stability. However, pure PDMS has very little use as a toughening agent. Due to its extreme incompatibility with epoxy resins, it is either macroscopically immiscible or exudes from the crosslinking matrix during curing procedure.

Therefore it was attempted in this work to compatibilize epoxy immiscible PDMS with epoxy miscible polycaprolactone (PCL) segments, which are attached as blocks to both PDMS endgroups. These hydroxy-terminated PCL-*b*-PDMS-*b*-PCL and (PCL)<sub>2</sub>-*b*-PDMS-*b*-(PCL)<sub>2</sub> block copolymers were synthesized with controlled microstructures, i.e., controlled block length, PCL content, and hydroxy functionality and are fully miscible with the uncured epoxy resin/curing agent mixture. During network formation in the curing process these block copolymer liquid rubbers undergo phase separation and form discrete microphases. Since the size of these microphases in the range of 20 nm is far below the wavelength of visible light, the cured resins are

\* To whom correspondence should be addressed.

† Present address: Gurit-Essex AG, CH-8807 Freienbach, Switzerland.

still transparent or at least translucent. Synthesis as well as morphology of these polysiloxane-modified epoxies are described in detail elsewhere.<sup>1</sup>

Since the purpose of the development of novel modifiers for epoxy resins is toughness enhancement without major losses in other mechanical properties of the resulting systems, the silicone-modified resins have been characterized mechanically. Standard measurements of short time strength and fracture toughness as well as impact testing have been performed. These investigations will be described in detail in a separate publication.<sup>2</sup> In addition to the short time mechanical behavior, it is essential in engineering design also to know the long-term strength and its governing parameters of these resins. In this study the slow crack growth behavior of epoxy resins, unmodified and modified with different amounts of (PCL)<sub>2</sub>-*b*-PDMS-*b*-(PCL)<sub>2</sub>, are investigated by direct measurements and fractographically with respect to strength and lifetime under static fatigue conditions.

## EXPERIMENTAL

### Materials

The toughening agent used in this investigation is a branched block copolymer (PCL)<sub>2</sub>-*b*-PDMS-*b*-(PCL)<sub>2</sub> with a PCL content of 48 wt % and a molecular weight  $M_n$  of 8000 g/mol.<sup>1</sup> The base resin GY 250 is a low-molecular-weight viscous bisphenol-A-diglycidylether resin, supplied from Ciba-Geigy AG, Basel. Its average molecular weight is 370–380 g/mol. Hexahydrophthalic acidanhydride HT 907 from Ciba-Geigy was used as curing agent in the presence of *N,N*-dimethylbenzylamine accelerator. For curing, the epoxy resin and the anhydride curing agent in a ratio 4 : 3 with various amounts of liquid rubber (in this case 0, 5, 10, or 15 wt %) were mixed thoroughly at 80°C and degassed under vacuum until bubble-free mixtures were obtained. Then 1 wt % accelerator was added carefully, and the mixture was poured into prewarmed (80°C) molds, where the curing mixture was heated at a rate of 2 K/min to 150°C. This temperature was held for 3 h and, after further heating, 180°C was held for another hour.

Syntheses and characterization of the polycaprolactone-compatible silicone liquid rubbers have been described previously.<sup>1</sup>

### Specimens

For the uniaxial tensile experiments, short-term tests as well as creep tests, dogbone-shaped tensile

bars according standard DIN 53 455 with 4 mm thickness, 10 mm width, and 50 mm gauge length have been used. These specimens were prepared by casting the resin in molds having the precise shape and size. The specimen edges were machined after curing by milling to remove burrs and notches caused by bubbles in the surface region.

The fracture mechanics experiments, measurement of fracture toughness and of crack speed functions, were performed using miniature compact tension (CT) specimens with the following dimensions: thickness  $D = 4$  mm, width  $W = 8$  mm, height  $2H = 8$  mm. The CT specimens were cut from plates molded together with the tensile bars. The initial crack was introduced as a saw cut, sharpened subsequently with a razor blade and then enlarged by dynamic fatigue to obtain a natural crack. Fatigue crack growth was controlled by direct observation in a microscope. As the unmodified epoxy resin is very brittle, exhibiting the tendency to uncontrolled crack propagation under dynamic fatigue at room temperature, the fatigue process of this material was performed successfully at elevated temperatures just below the glass transition temperature.

### Testing Methods

Short-term tensile properties such as strength and Young's modulus were measured according to the standard DIN 53 455 in a servohydraulic testing machine equipped with a 10 kN tensile load cell. The experiments were performed at a crosshead speed  $v = 5$  mm/min. A strain gauge extensometer was applied to measure longitudinal strains. The load and displacement were recorded simultaneously. The Young's modulus was taken from the initial linear region of the stress-strain curve.

Long-term creep tests were performed in a Franck creep testing system in which 15 tensile specimens can be loaded individually at constant loads. The loading device of each specimen was equipped with digital clocks indicating the loading time to an accuracy of 1/100 or 1/10 of an hour and having a circuit breaker to stop in the moment of specimen failure. Thus the lifetime of the specimens was measured as a function of fracture stress.

The crack propagation behavior of the differently modified epoxies was measured at room temperature with CT specimens in a testing apparatus for interferometric measurements of crack tip features as described in detail elsewhere.<sup>3</sup> This system enables direct observation of the propagating crack during slow crack growth under constant load. Thus, the load as well as a change in crack length with time

can be measured simultaneously. The crack growth controlling parameter, the stress intensity factor,  $K_I$ , can be determined at every crack speed with the respective load,  $F$ , and crack length,  $a$ , using the equation

$$K_I = \frac{2W + a}{D(W - a)^{3/2}} FY \quad (1)$$

with the geometry factor  $Y$  and the specimen dimensions  $D$ ,  $W$ . In connection with the crack growth experiments, interferometric micrographs of the crack tip region of some specimens were taken in this apparatus.

For the measurement of fracture toughness  $K_{Ic}$ , the CT specimens were loaded in the same apparatus at room temperature at a constant displacement rate (1 mm/min) until fracture occurred. During the test the load deflection curve was recorded with an X-Y plotter. These curves exhibited for all epoxy resins tested a nearly linear shape up to failure indicating almost linear elastic behavior without significant slow crack growth during the experiments. Hence the maximum loads and initial crack lengths could be taken to calculate  $K_{Ic}$  using Eq. (1).

Some fracture surfaces from the above experiments were examined in a scanning electron microscope (SEM), which were coated previously by sputtering with copper metal to achieve a conducting and protecting layer.

## RESULTS AND DISCUSSION

### Mechanical Properties of the Epoxy Resins with Different Modifier Content

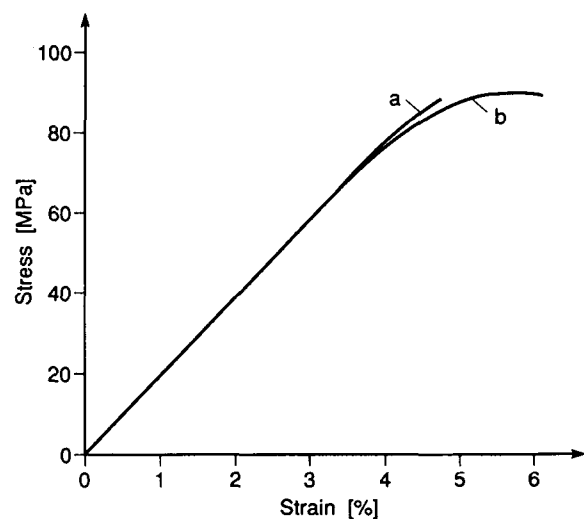
Addition of polycaprolactone-compatible silicone rubber (PDMS-*b*-PCL), especially branched triblock copolymer of the type (PCL)<sub>2</sub>-*b*-PDMS-*b*-(PCL)<sub>2</sub>, to epoxies before curing increases the toughness of the resulting resins. In the present case the dynamic toughness of the pure epoxy resin, measured as impact fracture energy of unnotched standard bend specimens (DIN 53 453),  $a_n = 380$  mJ increased by a factor of almost 3 by adding 5 wt % of the toughener, and remained unchanged in case of further increase of toughener content. Also the static fracture toughness  $K_{Ic}$  increased with addition of a small amount of toughener (5 wt % PDMS-*b*-PCL) by a factor of more than 2 (from 0.67 to 1.52 MPa  $\times \sqrt{m}$ ). With increasing toughener content there was a further moderate increase in  $K_{Ic}$  to 1.62 MPa  $\times \sqrt{m}$  (10 wt % PDMS-*b*-PCL) and

1.85 MPa  $\times \sqrt{m}$  (15 wt % PDMS-*b*-PCL), respectively.

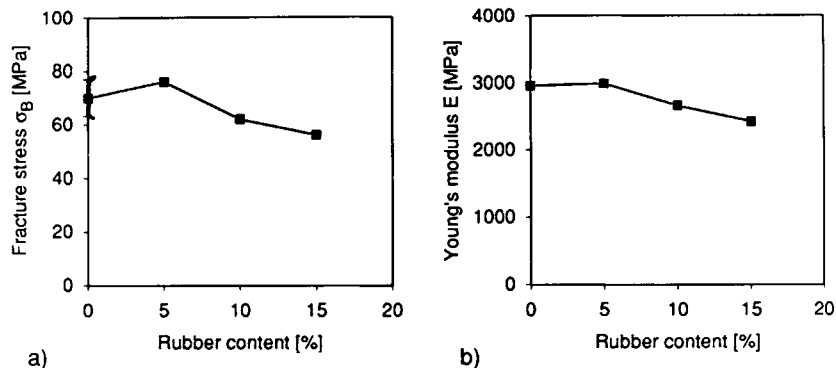
It is a well-known phenomenon that usually toughening of brittle polymers is accompanied by undesirable losses of strength and stiffness. Therefore a particular goal of developing advanced toughening systems is to achieve a synergistic combination of increased toughness and high strength and modulus. These mechanical parameters of the unmodified resin and of toughened resins with 5, 10, and 15 wt % PDMS-*b*-PCL rubber content were measured in tension according to the method described above.<sup>4</sup>

Figure 1 shows two typical stress-strain curves of epoxy resins, an unmodified and a toughened grade, demonstrating clearly increased fracture strain  $\epsilon_B$  of the modified material. From the respective curves strength, as fracture stress, and Young's modulus, as the slope of the stress-strain curve in the origin, were taken and compiled in Figure 2 as functions of rubber content. Each data point represents the average of several experiments. It has to be noted that in the case of the unmodified resin there was a large scatter in fracture stress, as indicated in Figure 2(a). This is due to the distribution of preparation-caused flaws in this brittle and, hence, notch-sensitive material.

The strength  $\sigma_B$  of the unmodified epoxy resin is about 80 MPa and its modulus  $E = 3000$  MPa, which are typical values for such a highly crosslinked polymer. Both strength and modulus of the resin are almost unchanged by the addition of 5 wt % tough-



**Figure 1** Stress-strain curves of an (a) unmodified (a) and (b) a modified epoxy resin with 5% PDMS-PCL content.



**Figure 2** Mechanical properties of epoxy resins as functions of modifier content: (a) tensile strength and (b) Young's modulus.

ening agent. For the higher rubber contents both of these parameters decrease with increasing amounts of the toughening agent. However, the values of  $\sigma_B = 62$  MPa or 56 MPa [10 or 15 wt % toughening agent, respectively; see Fig. 2(a)] and of  $E = 2700$  or 2400 MPa [Fig. 2(b)] are still of a comparable magnitude as those of the original material.

From dynamical-mechanical analysis the glass transition temperatures  $T_g$  have been determined, a measure for the suitability of the materials at elevated temperatures. Up to rubber contents of 10 wt % no decrease of the  $T_g = 120^\circ\text{C}$  of the nonmodified resin was detected. For 15 wt % toughener a slightly lower  $T_g$  of  $114^\circ\text{C}$  was measured.

The mechanical and thermal parameters characterizing the silicone-modified epoxy resins are compiled in Table I. These data illustrate that a significant enhancement in toughness was achieved with a toughening agent content as little as 5 wt % accompanied with minor increase for larger silicone rubber content. The short time mechanical properties, however, do not deteriorate significantly up to 10–15 wt % content of the toughening agent. These encouraging results concerning the short time behavior of the PDMS-*b*-PCL modified epoxies had to be complemented by the respective long-term re-

sults to prove the synergism of the different material's properties.

#### Long-Term Strength and Lifetime under Constant Load

For the application of materials in structures that have to bear load, the knowledge of the long-term strength measured as the time-dependent fracture stress is of essential interest. The long-term behavior of two silicone-modified epoxies (5 and 10 wt % PDMS-*b*-PCL, respectively) and of the unmodified resin were characterized by creep testing of the tensile specimens as described above. The specimens were subjected to different loads below the respective load leading to fracture in the short time experiments. Especially in the case of the unmodified epoxy resin the specimen edges had to be machined very carefully, because even small flaws led to a significant drop in strength in the short time tensile tests and, thus, to much shorter lifetimes in the creep experiments.

The fracture stress  $\sigma_B$  versus lifetime  $t_L$  of the three resins under investigation in the creep tests is plotted in Figure 3 in a log-log scale. All of the points show results of individual measurements.

**Table I** Material Parameters of an Epoxy Resin Modified with Different Amounts of a PDMS-*b*-PCL Modifier

PDMS- <i>b</i> -PCL (wt %)	$T_g$ ( $^\circ\text{C}$ )	$a_n$ (mJ)	$K_I$ (MPa $\times \sqrt{\text{m}}$ )	$\epsilon_B$ (%)	$\sigma_B$ (MPa)	$E$ (MPa)
0	120	380	0.67	3.0	82	2960
5	121	910	1.52	4.6	76	2990
10	121	940	1.63	4.0	62	2660
15	114	880	1.85	3.9	56	2420

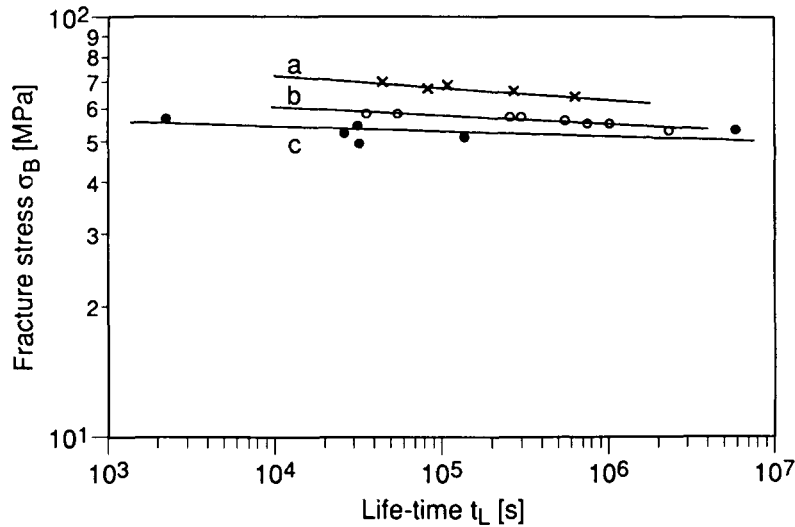


**Figure 3** Time dependence of fracture stress of epoxy resins: (a) unmodified and modified with (b) 5% and (c) 10% PDMS-PCL liquid rubber.

Based on these data points the shown regression lines according to equation

$$\log \sigma_B = \log B + m \log t_L \quad (2)$$

are calculated. The parameters  $B$  and  $m$  are listed in Table II.

Parameter  $B$  representing the intersection with the ordinate axis is the short time fracture stress at 1-s loading time. Thus, it should be comparable to the corresponding values in Table I. This holds for the modified resins quite reasonably. For the unmodified epoxy, however, the value of  $B$  is much higher than  $\sigma_B$ , indicating that in the short time experiments manufacturing induced flaws in specimens of this very notch-sensitive resin have significantly reduced the measured strength.

The fracture stress decreases slowly with loading time for the neat as well as for the toughened epoxies. The calculated regression functions have almost the same slope for the three differently modified

resins, although it seems to become smaller with increasing modifier content. For brittle polymers the slope of the lifetime function has been found to be governed by the crack growth behavior of the material, and that in this case the latter can be used for lifetime predictions.<sup>5,6</sup> Thus the similarity of the slopes of the lifetime functions of the three different materials may suggest similar crack growth behavior.

### Slow Crack Growth as a Lifetime Governing Mechanism

In order to check this hypothesis the crack growth behavior of the unmodified and modified epoxies was measured directly. Crack velocities between  $10^{-5}$  and  $10^{-2}$  mm/s in CT specimens under static load could be measured by direct observation of the crack tip in the interference optical microscope. According to the empirical function

$$da/dt = AK_I^n \quad (3)$$

which becomes linear if expressed as

$$\log da/dt = \log A + n \log K_I \quad (4)$$

the measured crack speed  $da/dt$  in an epoxy modified with 5 wt % PDMC-*b*-PCL is plotted logarithmically as a function of logarithmic stress intensity factor  $K_I$  in Figure 4.

Two distinct regions of this curve can be distinguished: The slope  $n$  of the regression line for crack

**Table II** Slope  $m$  and Intersection  $B$  of the Fracture Stress Versus Lifetime Functions of Differently Modified Epoxy Resins

PDMS- <i>b</i> -PCL (wt %)	$B$ (MPa)	$m$
0	92.2	-0.026
5	73.3	-0.020
10	61.2	-0.012

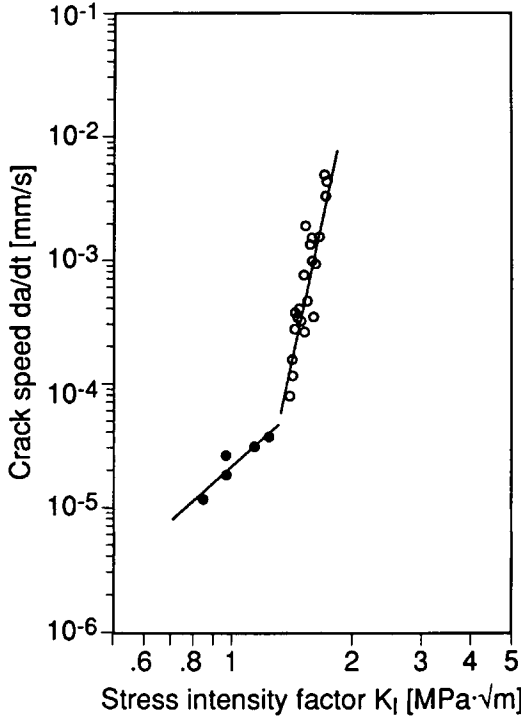


**Figure 4** Crack speed  $da/dt$  as a function of stress intensity factor  $K_I$  in an epoxy resin modified with 5% PDMS-PCL.

speeds above  $5 \times 10^{-5}$  mm/s is 16.3 while in the very slow crack speed regime below it is only 2.8. In the flat part of the curve below  $da/dt = 5 \times 10^{-5}$  mm/s the effect of stress relaxation exceeded the effect of crack length on the stress intensity factor  $K_I$  defined by the basic equation

$$K_I = \sigma \times \sqrt{a} \times Y \tag{5}$$

leading to a deceleration in crack speed. Therefore the values in this part of the curve should be neglected for further considerations.

The measured curve for the toughened epoxy with 10 wt % PDMS-*b*-PCL content shows a somewhat smaller slope of  $n = 10.8$  without a distinguishable transition in slope but with a larger scatter in the values.

For the unmodified epoxy experimental difficulties arose due to the brittleness of the material. Although slow crack growth could be observed in the microscope, reliable measurements of crack speed in the miniature CT specimens used were impossible due to fast acceleration in the crack propagation indicating a high value of  $n$ . Therefore a published function of crack propagation in an unmodified

epoxy resin was taken from the literature.<sup>7</sup> This curve exhibits a very steep slope of  $n = 45$  making the brittleness of the material evident.

The three functions of crack speed  $da/dt$  in epoxies versus stress intensity factor  $K_I$  are compiled in Figure 5. While the curves for the toughened grades are close together, differing only somewhat in slope, the curve for the unmodified grade is much steeper and shifted to lower stress intensity values. This correlates well with the much lower critical fracture toughness value of  $K_{Ic} = 0.67 \text{ MPa} \times \sqrt{\text{m}}$  of the pure epoxy compared to the  $K_{Ic}$  values of about  $1.6 \text{ MPa} \times \sqrt{\text{m}}$  for the toughened resins, measured in independent experiments.

Crack growth behavior and long-term strength of materials are closely related if the lifetime is mainly determined by the time of crack growth, starting from an initial crack length  $a_0$  up to some critical size. This time  $t_s$  of slow crack growth depends on the crack speed versus  $K_I$  function [Eq. (3)], which can be transformed<sup>5</sup> by integration in combination with Eq. (5) to

$$t_s = \frac{2a_0^{(2-n)/2}}{f^n A (n-2)} \sigma^{-n} \tag{6}$$

where  $f$  is a geometry-dependent proportionality factor. For several brittle polymers  $t_s$  can be taken as the lifetime.<sup>5,6</sup> The parameters  $n$  and  $B$  of Eq. (2) are correlated to those of Eq. (6) by

$$m = -1/n \tag{7}$$

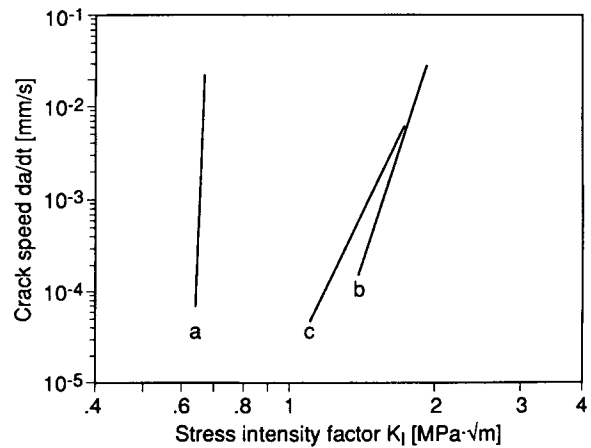


**Figure 5** Crack speed  $da/dt$  as functions of stress intensity factor  $K_I$  in epoxy resins: (a) unmodified and modified with (b) 5% and (c) 10% PDMS-PCL liquid rubber.

and

$$B = \left( \frac{2a_0^{(2-n)/2}}{f^n A (n-2)} \right)^{1/n} \quad (8)$$

The lifetimes of loaded specimens and subsequently also of other structures made from materials of this type can be predicted by this fracture mechanical approach from the acting stress  $\sigma$  using the parameters in the respective crack speed functions.<sup>5</sup>

Converting according to Eq. (7) the slopes of the crack speed functions in Figure 5 into slopes of lifetime functions the values listed in Table III are found. The calculated slope of the lifetime function ( $-1/n$ ) of the unmodified epoxy agrees quite well with the measured one ( $m$ ) as listed in Table II. This was to be expected for a brittle epoxy resin similar to those described in the literature.<sup>6</sup> The toughened grades, however, exhibit smaller slopes of the crack speed functions leading to too steep predicted lifetime curves.

The disagreement between measured and calculated slopes for the toughened epoxies may have different reasons. Taking the measured crack speeds as initial crack speed during the creep experiments, only short lifetimes much below  $10^{-5}$  s are covered. Thus, the extrapolation to much slower crack growth rates, which is implied for longer lifetimes, seems to be invalid. This may be due to a change in the crack speed function for lower speeds. Another possibility is that in this case the time of slow crack growth is only a portion of the lifetime and that also other processes such as crack initiation or time-dependent plastic deformation do contribute to the lifetime of these materials under load. Also time-dependent crack tip blunting mechanisms may affect the crack growth behavior leading to an overestimation of the  $K_I$  values during crack propagation. The latter possibility can be examined by interferometric investigations of crack tip micromechanics.

### Effect of Toughening on Micromechanics of Fracture

Dispersed rubbery particles in a rigid polymer matrix act as stress concentrators. If loaded, they cause a large number of localized subcritical deformation zones consuming much energy and, thus, increasing the toughness of the system. Such a general toughening mechanism may act by different deformation mechanisms, such as crazing, shear yielding, or cavitation, having also different effects on the crack propagation behavior.

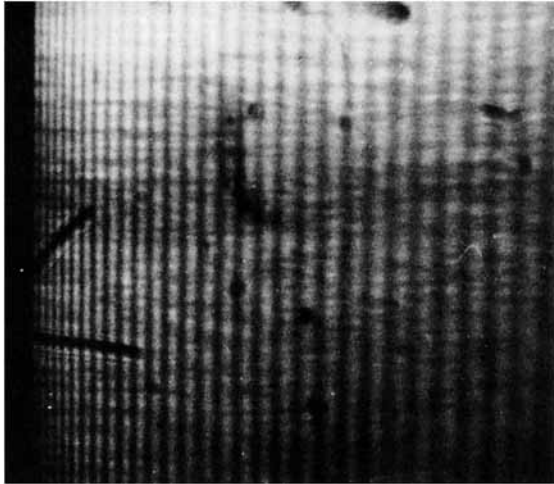
**Table III Slopes  $n$  of Crack Speed Functions of Differently Modified Epoxies and Derived Slopes ( $-1/n$ ) of the Predicted Lifetime Functions**

PDMS- <i>b</i> -PCL (wt %)	$n$	$-1/n$
0	45	-0.022
5	16.3	-0.061
10	10.8	-0.093

In the present PDMS-*b*-PCL toughened epoxies, the phase-separated liquid rubbery toughening agent is distributed homogeneously as particles of about 20 nm diameter, as was observed by transmission electron microscopy (TEM).<sup>1</sup> The macroscopic effect of the particles becomes evident in Figure 1, increasing the strain to fracture and, hence, also the fracture energy. The microscopic effects, however, must be investigated by micromechanical measurements.<sup>8</sup>

Since the crack propagation measurements were performed in an interferometric setup, the special facilities of this apparatus<sup>3</sup> have been used to measure the crack tip deformation in the resins investigated. Micrographs of the interference fringe patterns of the light reflected on the crack surfaces near the tip in the CT specimen were taken at different load levels. Figure 6 shows as an example the interference fringe pattern from a specimen of unmodified epoxy resin loaded slightly below the critical stress intensity factor  $K_{Ic}$  (fracture toughness). It is a single pattern from the crack opening without any indication of another pattern in front of the crack tip. This indicates that if the size of the possible deformation zone is above the resolution of the microscopical system, it cannot be a craze zone, which would also create interferences.

To evaluate the crack opening, the order number of the individual fringes has to be known. If there is some crack tip displacement due to plastic deformation (crack opening stretch, COS), the first fringe at the crack tip has an unknown order number. This number can be determined by counting the fringes that disappear in the crack tip during increasing load. However, there is still some uncertainty in the order number since also in the unloaded state a remaining plastic zone may cause some crack tip displacement. Thus the estimated fringe order can be somewhat too low. In the fringe pattern shown, the first fringe (slightly in front of the crack tip) has an estimated order number 10. The measured crack contour in an unmodified epoxy taken from Figure



↑  
Crack Tip

**Figure 6** Interference fringe pattern from light ( $\lambda = 546$  nm) reflected on the fracture surfaces near the crack tip in an unmodified epoxy resin.

6 and a similar contour in an epoxy modified with 5 wt % PDMS-*b*-PCL, also loaded slightly below  $K_{Ic}$  for this material, are shown in Figure 7. The COS values estimated by extrapolation of the crack contours to the crack tip are 2.4 and 5.8  $\mu\text{m}$ , respectively.

COS as well as crack opening displacement (COD) along the crack are significantly larger in the toughened material. This reflects an increased plastically deformed volume before crack growth and, hence, also an increased toughness in the toughened epoxy resin. A larger compliance due to a reduced elastic modulus seems not to be the case as may be taken from the similarity of the  $E$  values as listed in Table I.

Applying basic fracture mechanics,<sup>9</sup> the stress intensity factor  $K_I$  can be determined micromechanically using equation

$$K_I = 2v(r)E\sqrt{r} \times \text{const.} \quad (9)$$

from the local displacement  $2v(r)$  (COD) in the distance  $r$  from the crack tip. Since there is a factor of about 2 between the respective COS (and similarly between COD) for the two different grades of epoxy shown in Figure 7, the acting stress intensity factor must have a comparable ratio that proves the previously measured fracture toughnesses of the respective materials. Thus also for cracks in the toughened material the linear elastic approach is still valid, at least for short loading times. For longer times, e.g., for creep conditions, the possibility of blunting effects is still to be investigated.

### Fractographic Observations

The large deformations in front of the propagating crack in a toughened polymer should be reflected by their remnants on the fracture surface.<sup>10</sup> Since the crack growth process in the experiments described above was observed directly, the markings on the fracture surfaces created in the CT specimens can be correlated to the proper type of fracture.

An SEM micrograph of such a fracture surface in toughened (with 5 wt % PDMS-*b*-PCL) epoxy is given in Figure 8. Three different regions on the surface may be distinguished: The regions on the top and the bottom of the micrograph are almost structureless while in between there is a region with evident signs of plastic deformation. The upper structureless regime is the area of fatigue crack growth during generation of the starter crack. Below the fatigue fracture surface the area of slow crack propagation follows. This is a zone of large crack tip deformation (compare Fig. 7). The markings indicate that the crack propagated in slightly different planes, causing the highly deformed steps parallel to the crack growth direction. This may be explained by fluctuation in strength of the plastically deformed matter in front of the blunted crack tip, causing several starting points of crack growth along the crack front. The markings parallel to the crack front are arrest lines or signs of discontinuous changes in crack speed indicating the positions of the individual measurements. The transition from slow to fast crack propagation (from region b to c on Fig. 8) is marked again by a distinct line. After this line (on the picture below the line) major plastic deformations disappear, indicating the crack speed (strain rate) induced embrittlement of the polymer. Further on the crack planes unify in a single one proceeding

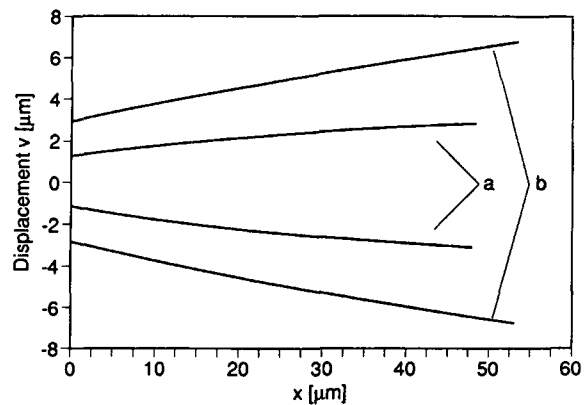


**Figure 7** Interferometrically measured crack tip contours in an (a) unmodified epoxy resin (compare Fig. 6) and in (b) a toughened (5% PDMC-PCL) resin.



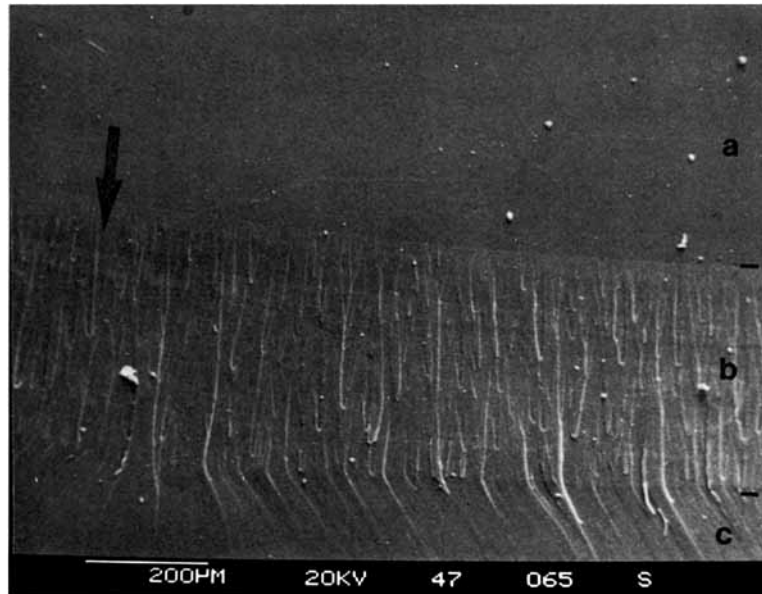


**Figure 8** SEM of a fracture surface on a CT specimen of a toughened epoxy resin (5% PDMS-PCL) exhibiting the regimes of (a) fatigue crack growth, (b) slow (controlled) crack propagation, and (c) uncontrolled (fast) failure. Crack propagation direction is indicated by an arrow.

from a sharp crack tip with very small deformations. Marks of the rubbery inclusions, as known from CTBN-modified epoxies,<sup>11</sup> cannot be seen in either region of the fracture surface. This is due to their small dimensions below the resolution of the SEM.

The fracture surface of an unnotched tensile

sample of the same material (5 wt % PDMS-*b*-PCL) is shown in Figure 9. Regimes of subcritical (in an almost semicircular region) as well as of fast crack growth are visible. The crack started from a defect in the interior of the specimen, apparently being a cluster of foreign material or of an aggregate of elas-

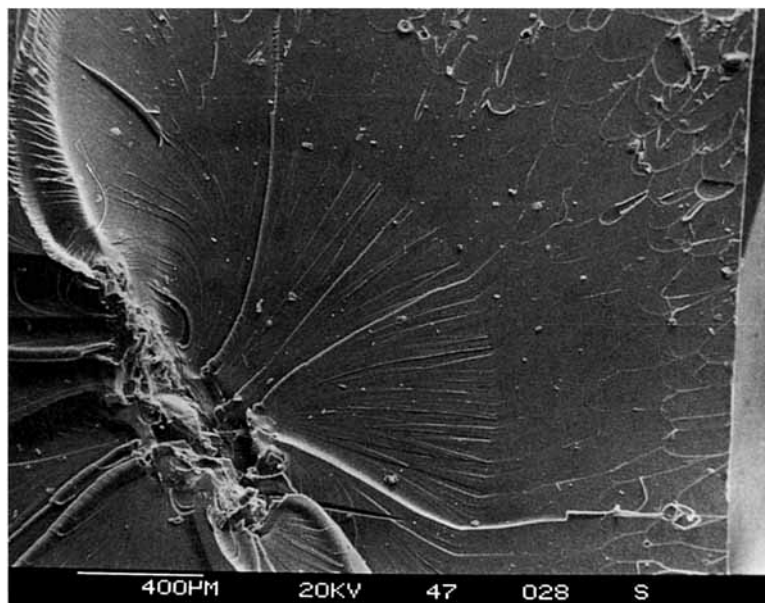


**Figure 9** SEM of a fracture surface on a tensile specimen of a 5% PDMS-PCL modified epoxy resin;  $\sigma_B = 59$  MPa,  $t_L = 3.34 \times 10^4$  s.

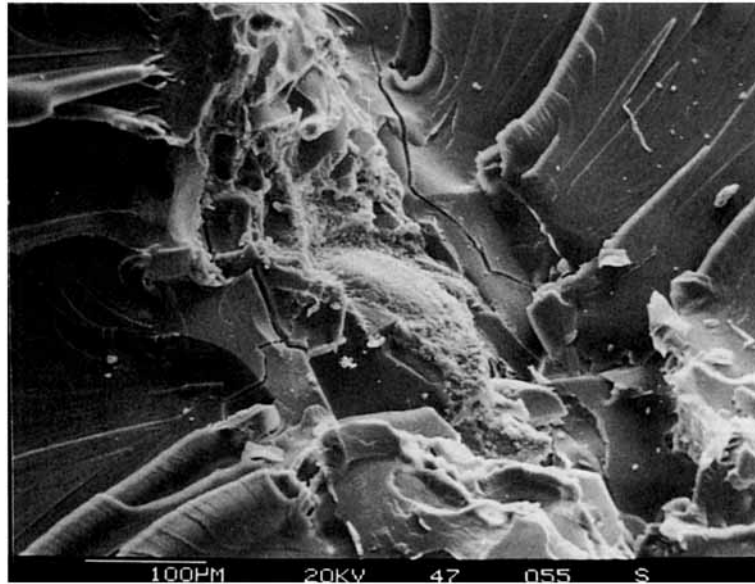


**Figure 10** SEM of the crack origin in Figure 9 at higher magnification.

tomic particles, as can be seen at a larger magnification in Figure 10. The initiation site is surrounded semicircularly by a smooth region where the stable crack growth took place. During proceeding crack propagation, probably with increased plastic zone at the crack tip, the deformed steps in crack propagation direction occur as also can be seen on the fracture surface of the CT specimen. A sharp line marks the transition to fast crack growth. The

region of unstable crack growth is first smooth like on the CT specimen, later on, however, it increasingly becomes rougher. In contrast to the CT specimens, where the maximum crack speed of the respective material normally cannot be reached because of too long initial notches, in not pre-notched specimens under the creep testing conditions crack speed increases to larger magnitudes. This may cause surface roughness by the generation of secondary

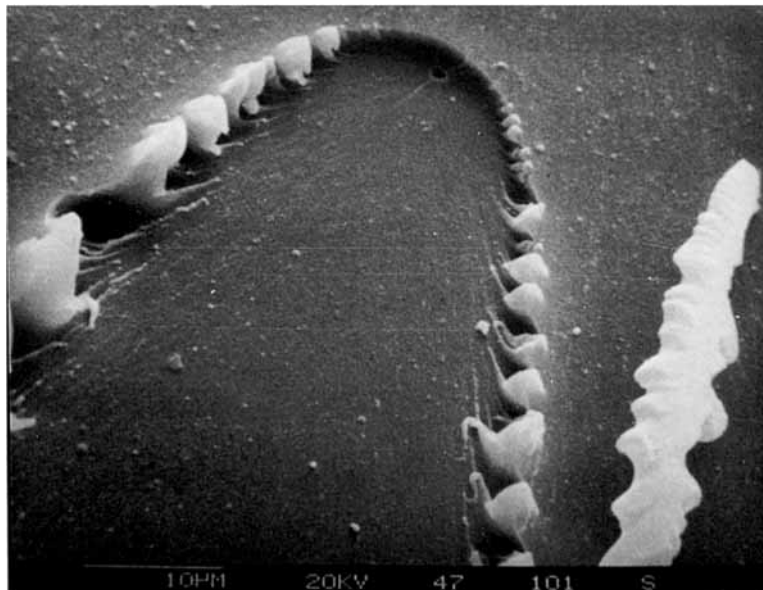


**Figure 11** SEM of the parabolic marking originating from a secondary crack. Detail of Figure 9 at higher magnification.

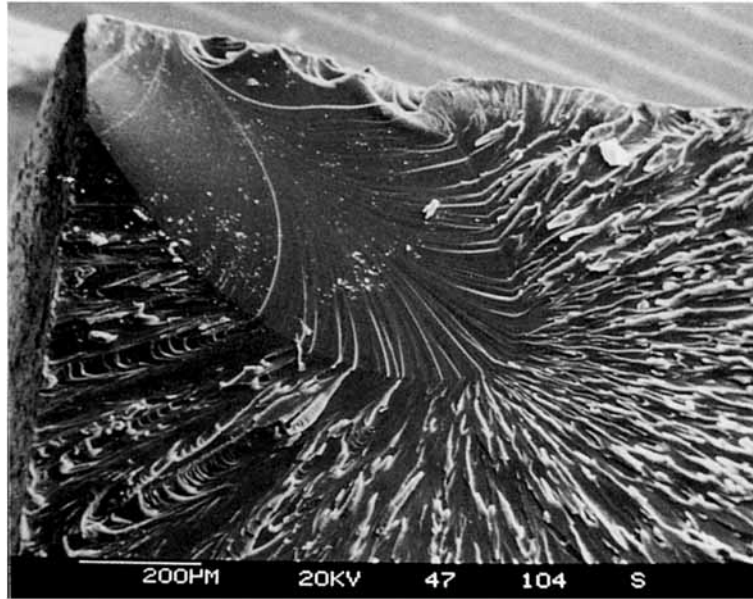


**Figure 12** SEM of a fracture surface on a tensile specimen of an unmodified epoxy resin;  $\sigma_B = 70 \text{ MPa}$ ,  $t_L = 4.2 \times 10^4 \text{ s}$ .

cracks at inhomogeneities in the resin and their subsequent combination with the main crack. In Figure 11 at a higher magnification the micrograph of the parabolic front of a secondary fracture starting from void with a diameter of about  $1 \mu\text{m}$  illustrates the large deformation occurring between the approaching crack planes.

Comparing a fracture surface of the unmodified epoxy shown in Figure 12 some differences become evident. The crack originates from some damage at the specimen surface, as can be seen more clearly from the higher magnification of this area in Figure 13. The slow crack growth region has in this case an elliptical form with a fracture surface similar to

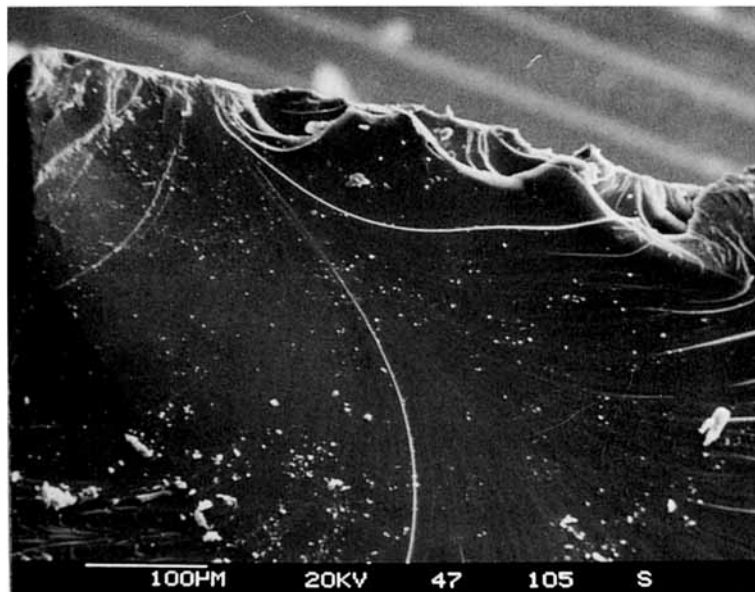


**Figure 13** SEM of the crack origin in Figure 12 at higher magnification.

the respective area of the modified epoxy. In the fast crack growth regime, however, roughness starts directly at the transition line indicating an almost immediate acceleration to the final crack speed.

## CONCLUSIONS

The use of PDMS compatibilized with end groups of block PCL with the basic structure  $(PCL)_2$ -*b*-PDMS-*b*- $(PCL)_2$  as a toughening agent for epoxy resins leads to phase-separated systems with uniformly dispersed elastomeric particles in the order of magnitude of 20 nm. For this system with different modifier contents the following main properties have been found:

1. Transparency of the polymeric materials up to 10 wt % modifier content
2. Increase in toughness (impact as well as short time fracture toughness) by factors of more than 2 for toughener contents of 5 wt % or more
3. Almost unchanged short time mechanical properties (strength, *E* modulus) at a toughener content of 5 wt % and a moderate decrease for higher contents
4. Drastic drop in notch sensitivity of the toughened resins
5. Slight decrease in long-term strength with increasing toughener content
6. Time-dependent strength behavior of the unmodified epoxy can be described by the fracture mechanical approach of slow crack propagation, in the case of modified systems this approach is too conservative

The described toughening agent increases the toughness of the system remarkably even for low toughener contents. For low toughener contents a

basically synergistic effect in increasing toughness and almost unchanged mechanical properties is found. Thus it can be concluded that the *b*-PDMS-*b*-PCL is a most promising toughening agent for epoxy resins with most advantageous effects when employed in low concentrations.

The investigations described in this paper were performed within the Sonderforschungsbereich 60 supported by the Deutsche Forschungsgemeinschaft.

## REFERENCES

1. U. Buchholz and R. Mülhaupt, *ACS Polym. Prepr.*, **33**(1), 205 (1992).
2. U. Buchholz, W. Böhme, and R. Mülhaupt, to appear.
3. W. Döll and L. Könczöl, in *Crazing in Polymers*, Vol. 2, H. H. Kausch, ed., *Adv. Polym. Sci.*, **91/92**, Springer-Verlag, Berlin, 1990, p. 137.
4. U. Buchholz, Ph.D. Thesis, Universität Freiburg, 1992.
5. W. Döll and L. Könczöl, *Kunststoffe*, **70**, 563 (1980).
6. H. R. Beer, T. Kaiser, A. C. Moloney, and H. H. Kausch, *J. Mater. Sci.*, **21**, 3661 (1986).
7. R. J. Young and P. W. R. Beaumont, *J. Mater. Sci.*, **12**, 684 (1977).
8. W. Döll, L. Könczöl, and L. Bevan, in *Encyclopedia of Polymer Science and Engineering*, Vol. 9, 2nd ed, Wiley, New York, 1987, p. 745.
9. G. R. Irwin, "Fracture," in *Handbuch der Physik*, Vol. 6, S. Flügge, Ed., Springer-Verlag Berlin, 1958, p. 551.
10. A. C. Roulin-Moloney, Ed., *Fractography and Failure Mechanisms of Polymers and Composites*, Elsevier Appl. Sci., London, 1989.
11. A. F. Yee and R. A. Pearson, in *Fractography and Failure Mechanisms of Polymers and Composites*, Elsevier Appl. Sci., London, 1989, p. 291.

Received September 2, 1993

Accepted May 10, 1994